# RADIOWAVE PROPAGATION IN MULTIPATH CHANNELS

With the rapid growth in wireless communications, there is considerable interest in radiofrequency (RF) propagation and RF channel modeling in the 400 MHz to 2 GHz band, where multipath propagation is a characteristic property. The topic of RF signal propagation and the factors that affect the RF signals have been extensively studied over the last few decades (1–3). This article presents a comprehensive overview of the RF signal variations related to propagation in multipath fading channels. The diverse phenomena that cause signal variations are described via mathematical models. The different types of fading and their salient features are discussed in detail. The goal of this article is to provide a mathematical and an engineering-oriented treatment of multipath fading, thereby providing the reader with the necessary tools and the information to understand the different RF propagative issues and how they impact wireless communications.

The different propagative effects are classified in two major categories as shown in Fig. 1:

- small-scale effects
- large-scale effects

The small-scale effects are those caused by multipath propagation, the phenomenon by which the transmitted signal reaches the receiver via multiple paths. The received signal is a superposition of the different multipath signals, which add constructively or destructively, thereby producing signal fluctuations. The variations of the signal level are typically produced by movement over short distances (10–20 times the wavelength $\lambda$ of the RF carrier) during which the mean signal level remains constant. The different types of fading and their mathematical characterization and modeling are discussed in the following sections.

On the other hand, large-scale effects are those caused by variations in the distance between transmitter and receiver, which are manifested in the form of path loss, and by environmental factors, such as terrain, which produce log-normal shadowing about the local mean signal level. These issues are also discussed in detail.

A schematic of a communication system is shown in Fig. 2. The term "channel" is used to imply different portions of the communication link. Two terms used in this article, namely, the propagative channel and the baseband channel need to be defined. The propagation channel is the physical medium that supports RF propagation between the transmitting and receiving antennas. This includes the objects that cause the multipath and time dispersion. This channel is time-varying. The baseband equivalent channel consists of a complex-valued baseband representation of the channel. If the nonlinearities in the IF/RF stages of both transmitter and receiver are neglected, then the baseband channel can also be represented by a linear, time-varying channel model, which includes the appropriate models for the propagation channel.

## BASIC DEFINITIONS

### Static Channels

The simplest type of communication channel is a static channel, in which the only signal impairment caused by the channel is additive white Gaussian noise (AWGN). The noise is assumed to have a flat, power-spectral density and is uncorrelated in time. These characteristics are typical of the thermal noise generated in communication equipment.

The AWGN channel is widely used to evaluate the performance of communication systems (4) (modulation, coding, etc.). In RF communications, a static environment is unlikely, except in a few situations when there is a dominant line-of-sight (LOS) component between the transmitter and receiver, and there is essentially no multipath, such as in microwave LOS links and in microcells. In practice, the AGWN channel serves the useful role of providing performance bounds for RF communication channels because the practical channels (typically Rayleigh and Ricean) always produce signal impairments more severe than the AGWN channel.

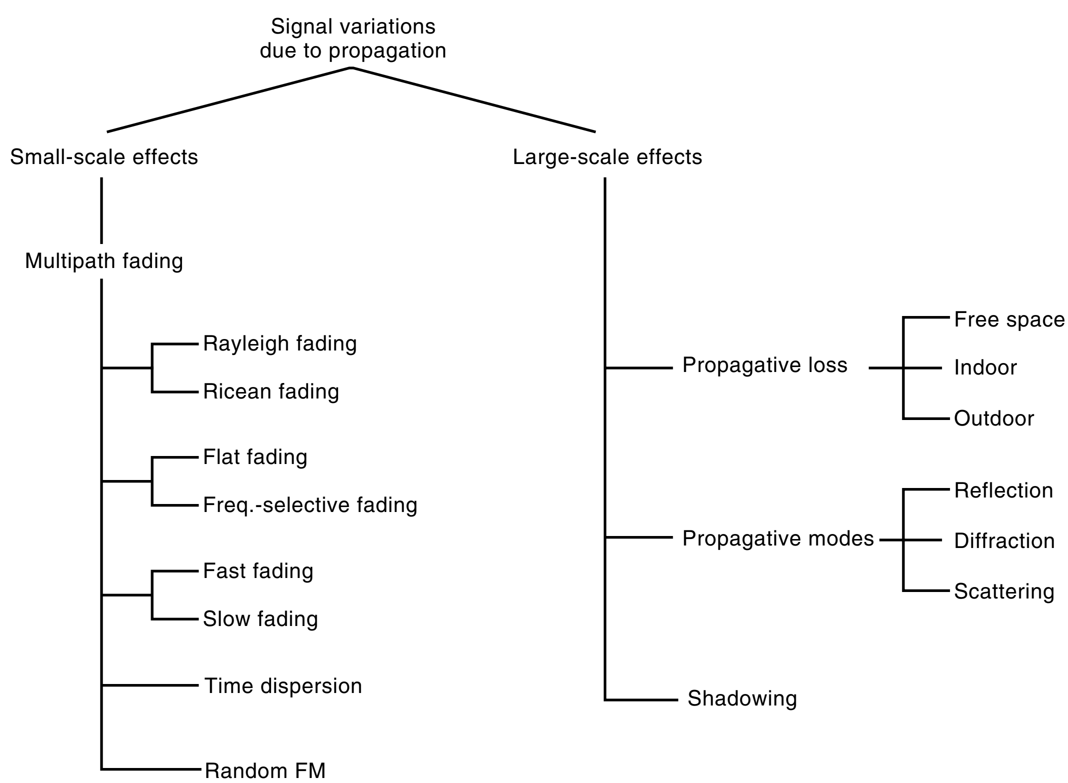


**Figure 1.** Classification of the small-scale effects and the large-scale effects that cause signal variability in an RF environment.

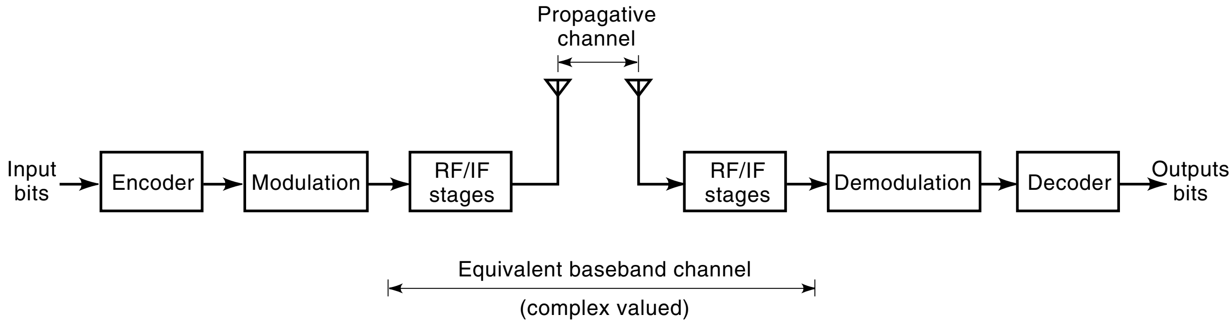


**Figure 2.** Definition of propagative channel and baseband channel.

### Fading Channels

Some of the commonly encountered communication channels, such as that encountered in wireline communications over telephone networks, can be characterized as AWGN channels that have a linear time-invariant (LTI) filter channel model. However, this representation does not apply to radio frequency (RF) channels because their transmission characteristics change with time and hence require statistical characterization using *linear, time-varying channel models.* Typically RF channels are characterized by the following time-varying phenomena:

1. multipath propagation and signal fading
2. multipath time dispersion
3. Doppler shift
4. random frequency/phase modulation
5. shadowing

In this article, these salient features of RF fading channels and their statistical characterization are described. Some examples of RF channels that fall under this category are

- mobile cellular channels
- mobile satellite channels
- channels with ionospheric and tropospheric propagation

**Multipath and Time Dispersion.** *Multipath* is the phenomenon by which a transmitted signal reaches a receiver via multiple propagative paths, each of which has an associated propagative delay. For instance, in Fig. 3, the signal from the base station to the mobile station has three paths with propagative delays $\tau_1$, $\tau_2$, and $\tau_3$, respectively. One of them is the direct line-of-sight path between the transmitter and receiver (with delay $\tau_1$). The other two paths (with delays $\tau_2$ and $\tau_2$) are caused by scatterers/reflectors. If a narrow pulse is transmitted in this channel (with $\tau_1 \neq \tau_2 \neq \tau_3$), then three copies of the pulse are received, as shown in Fig. 4. Channels exhibiting this property are called *time-dispersive.*

**Doppler Spread.** Another distinctive characteristic of radio channels is the time variation of the channel. This can be caused by mobility of transmitter or receiver or a change in the propagative environment (change in the scatterers). The received signal $x(t)$ in this time-varying multipath channel can be expressed as

$$x(t) = \sum_n \alpha_n(t) s[t - \tau_n(t)] \tag{1}$$

where $s(t)$ is the modulated signal, $\alpha_n(t)$ and $\tau_n(t)$ are the attenuation factor and the propagative delay, respectively, for the signal received via the $n$th path. The modulated signal $s(t)$ is typically represented as (4)

$$s(t) = m(t)\cos[2\pi f_c t + \theta(t)] = \mathrm{Re}[u(t)e^{j2\pi f_c t}] \tag{2}$$

with carrier frequency $f_c$, and $u(t) = m(t) \cos\theta(t)$ - $jm(t) \sin\theta(t)$. Substituting Eq. (2) in Eq. (1), the signal received $x(t)$ is given by

$$x(t) = \mathrm{Re}\left(\left\{\sum_n \alpha_n(t) e^{-j2\pi f_c \tau_n(t)} u[t - \tau_n(t)]\right\} e^{j2\pi f_c t}\right) \tag{3}$$

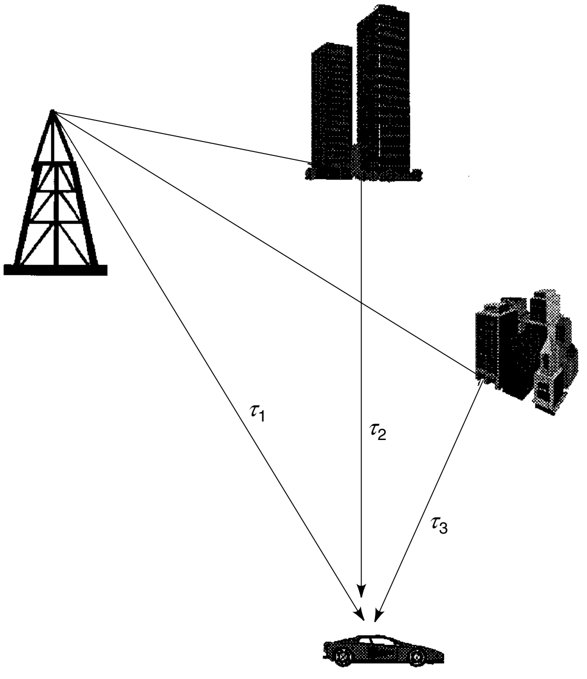


**Figure 3.** An example of multipath propagation due to multiple scatterers.

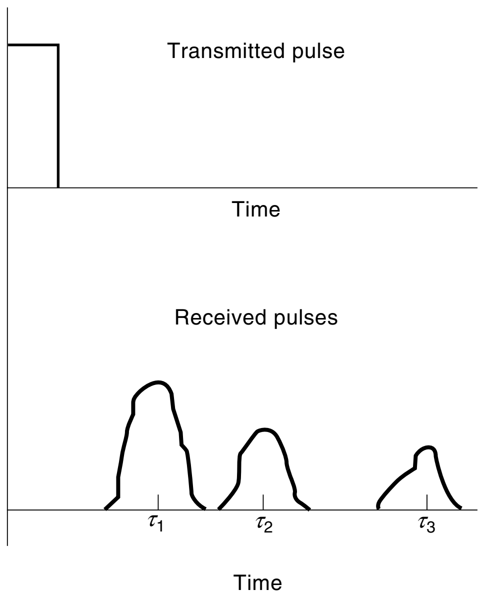


**Figure 4.** Effect of time dispersion due to multipath propagation.

The corresponding baseband (complex) signal $r(t)$ and the equivalent baseband channel $c(\tau;t)$ are given by

$$r(t) = \sum_n \alpha_n(t) e^{-j2\pi f_c \tau_n(t)} u[t - \tau_n(t)] \tag{4}$$

$$c(\tau;t) = \sum_n \alpha_n(t) e^{-j2\pi f_c \tau_n(t)} \delta[t - \tau_n(t)] \tag{5}$$

Consider the transmission of an unmodulated carrier $s(t) = A \cos 2\pi f_c t$. Then, using Eq. (4), with $u(t) = 1$, the received signal is given by

$$r(t) = \left[ A \sum_n \alpha_n(t) e^{-j2\pi f_c \tau_n(t)} \right] \tag{6}$$

which also represents the response of the channel to a complex exponential $e^{j2\pi f_c t}$. Even though $s(t)$ is a monochromatic signal, the output of the channel $r(t)$ contains many different frequency components, which are generated as a result of the time variations of the channel response. The range of frequencies over which the spectrum of $r(t)$ is non-zero is called the *Doppler frequency spread* ($B_d$) of the channel, which yields a measure that is directly proportional to the rate of variations of the channel response.

**Signal Fading.** In Eq. (5), $c(\tau;t)$ is the time-varying (complex-valued) channel impulse response (CIR) and is the discrete multipath channel model, wherein $\tau$ represents the time dispersion and $t$ denotes the time index for the variations as a function of time. The CIR $c(\tau;t)$ can be viewed as the superposition of phasors, each with a time-varying gain/amplitude $\alpha_n(t)$ and a time-varying phase $\phi_n(t) = -2\pi f_c \tau_n(t)$. With random variations in $\alpha_n(t)$ and $\phi_n(t)$ (caused by the time-varying multipath), these phasors can add constructively or destructively. The *fading phenomenon,* which results in signal amplitude becoming very small, is caused by instantaneous destructive combining of the phasors. An important observation is that a small change in $\tau_n(t)$ produces a significant phase change (i.e., a $2\pi$ change occurs if $\tau_n(t)$ changes by $1/f_c$). Using the central limit theorem, $r(t)$ can be modeled as a complex-valued Gaussian random process (4), which implies that $c(\tau;t)$ is also a complex-valued Gaussian random process in the $t$ variable. This random amplitude variation is a fundamental characteristic of multipath channels, and hence its understanding is crucial to the use of these channels. In *Rayleigh fading* channels, $c(\tau;t)$ is modeled as zero-mean, and corresponds to the case when there are random variations in the scattering environment (usually caused by the movement of the transmitter or receiver) and there is no line-of-sight (LOS) path. In *Ricean fading* channels, $c(\tau;t)$ is non-zero mean because of the presence of a LOS component or because of fixed scatterers. Typically Rayleigh fading channels are encountered in all cellular and land mobile radio communications, whereas Ricean fading channels are encountered in mobile satellite communications. A detailed characterization of these channels is presented in the subsequent sections.

In some cases, it is more suitable to have a continuous multipath model. In this case, the received signal $x(t)$ is given by

$$x(t) = \int_{-\infty}^{\infty} c(\tau;t) s(t-\tau)\, d\tau \tag{7}$$

which is similar to Eq. (1) with the summation replaced by an integral. This model is typically used in tropospheric scatter and ionospheric propagation. In the sequel, we focus on the discrete model for multipath channels, which is typical for most terrestrial RF channels.

**Fading in a Mobile Communication Environment.** If the transmitter and receiver were stationary and all the scatterers were fixed, then the signal fading variations, described in the previous section, would not be observed. In mobile communications (such as cellular), the receiver or transmitter is usually moving. So the scattering environment is constantly changing. A typical fading signal envelope (characterized by Rayleigh fading) for a mobile receiver using a carrier frequency $f_c$ = 1.9 GHz and moving at 100 km/h, is shown in Fig. 5. It can be seen that the signal envelope can vary as

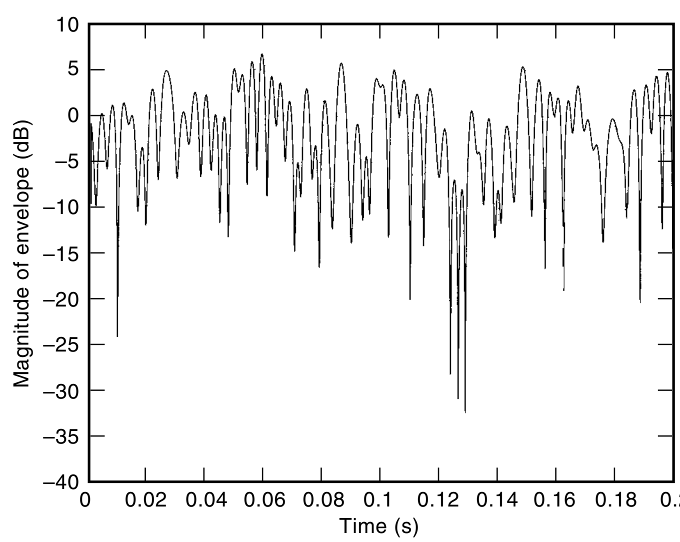


**Figure 5.** Typical envelope variations in Rayleigh fading at a vehicle speed of 100 km/h and carrier frequency 1.9 GHz. The rms value of the signal envelope is 0 dB.

much as 40 dB (30 dB below and 10 dB above) relative to the rms value.

A spatial viewpoint of multipath fading is very useful. Consider a stationary transmitter and fixed scatterers. The signals from the scatterers can be visualized as forming a spatial standing wave pattern with peaks (points in space where the multipath signals add constructively) and troughs (where the signals add destructively). The spatial separation between troughs and peaks is roughly $\lambda/2$, where $\lambda$ is the wavelength of the carrier. If a mobile receiver were to move through this spatial standing wave pattern, then it experiences the signal fading every time the receiver has moved by $\lambda/2$. In Fig. 5, the $x$-axis is the time in seconds. As the receiver moves, it can experience multiple signal fades per second.

***Example 1:*** Consider a mobile station moving at 100 km/h and communicating at a carrier frequency of 1.9 GHz. The corresponding wavelength $\lambda = 0.15$ m. Because the vehicle is moving at 100 km/h (= 27.77 m/s), the vehicle covers a distance corresponding to $176\lambda$ in 1 s. Hence, the envelope of signal received by the mobile can experience as many as 350 signal fades per second, as shown in Fig. 5. The extent of signal impairment depends on the extent of signal amplitude reduction, known as the *depth of the fade.* This is quantified via the level crossing rate and the duration of fades discussed in a subsequent section.

**Shadowing.** *Shadowing* is the term that refers to the long-term variations in the local mean of the received signal power at a distance $d$ from the transmitter. These variations are typically caused by the terrain, buildings, foliage, and other obstructions in the signal path. If the instantaneous power of the signal received at the receiver is averaged to remove the effect of fast fading, the local mean signal level $\Omega'$ at that particular distance $d$ from the transmitter is obtained. The local mean remains constant over a small distance (of the order of multiples of the wavelength of the RF carrier). The local mean $\Omega'$ is a random variable because of the signal level variations caused by the terrain and other environmental factors. Through empirical studies, the RV $\Omega'$ has been characterized by the log-normal distribution (see the next section) with a standard deviation in the typical range of 6 dB to 9 dB.

## FADING DISTRIBUTIONS

The two most commonly encountered types of fading environments are

1. Rayleigh fading
2. Ricean fading

In this section, the statistical properties of Rayleigh and Ricean fading are described. This mathematical framework is very useful in providing tools for analyzing and simulating the performance of communications over fading channels and also for providing insight into the design of robust communication systems in a fading environment (see Ref. 16). Ricean fading covers a very broad spectrum of environments from static AWGN channels on the one end to Rayleigh fading channels on the other. So, it represents an entire family of fading channels. However, because Rayleigh channels are the most frequently encountered environment in wireless (mobile) communications, it forms an important class for study. Both Rayleigh and Ricean distributions refer to the statistics of the received signal's envelope.

## RICE DISTRIBUTION

Let $X$ and $Y$ be two independent Gaussian random variables (RVs) with means $m_1$ and $m_2$, respectively, and common variance $\sigma^2$. Then the RV $V$, defined as $V \triangleq \sqrt{X^2 + Y^2}$, is distributed according to *Ricean distribution* (8), whose pdf is given by

$$f_V(v) = \begin{cases} \dfrac{v}{\sigma^2} I_0\left(\dfrac{sv}{\sigma^2}\right) e^{-\frac{v^2+s^2}{2\sigma^2}} & v > 0 \\ 0 & v \le 0 \end{cases} \tag{8}$$

where $s^2 = m_1^2 + m_2^2$ and $I_0$ is the zeroth order modified Bessel function of the first kind given by

$$I_0(x) = \frac{1}{2\pi}\int_0^{2\pi} e^{x\cos u}\,du = \frac{1}{2\pi}\int_{-\pi}^{\pi} e^{x\cos u}\,du \tag{9}$$

It can be verified that the RV $\hat{V} = V^2$ has a noncentral chi-square distribution whose noncentrality parameter is $s^2$. The cdf of a Ricean RV $V$ is given by (4)

$$F_V(v) = Pr(v \le V) = \int_0^V f_V(v)\,dv = 1 - Q\left(\frac{s}{\sigma}, \frac{v}{\sigma}\right) \tag{10}$$

where $Q$ is the generalized $Q$-function defined as

$$Q(a,b) = e^{-\frac{a^2+b^2}{2}} \sum_{k=0}^{\infty} \left(\frac{a}{b}\right)^k I_k(ab), \quad b > a > 0$$

and $I_k(x)$ is the $k$th-order modified Bessel function of the first kind.

Ricean fading is typically encountered in environments where there is a dominant, nonfading signal component (i.e., a line-of-sight path between transmitter and receiver, and this causes the nonzero mean of $X$ and $Y$). This is commonly true in mobile satellite channels. The signal received can be modeled as the superposition of the scattered multipath signals (with random angles of arrival) and the line-of-sight signal. The effects of the scattered signals depends on their strength relative to the strength of the nonfaded signal, which is characterized by the parameter called *Ricean factor K,* defined as $K \triangleq s^2/2\sigma^2$. It is quite common to specify the Rice factor in decibels, $K_{dB} \triangleq 10 \log_{10} K$ dB. As mentioned previously, the Ricean distribution spans a broad spectrum of fading environments, including the following special cases:

- $K \to 0$ ($\Rightarrow s^2 \sim 0$) $\Rightarrow$ Rayleigh fading channel
- $K \gg 1$ ($\Rightarrow s^2 \gg \sigma^2$) $\Rightarrow$ static channel (no fading)

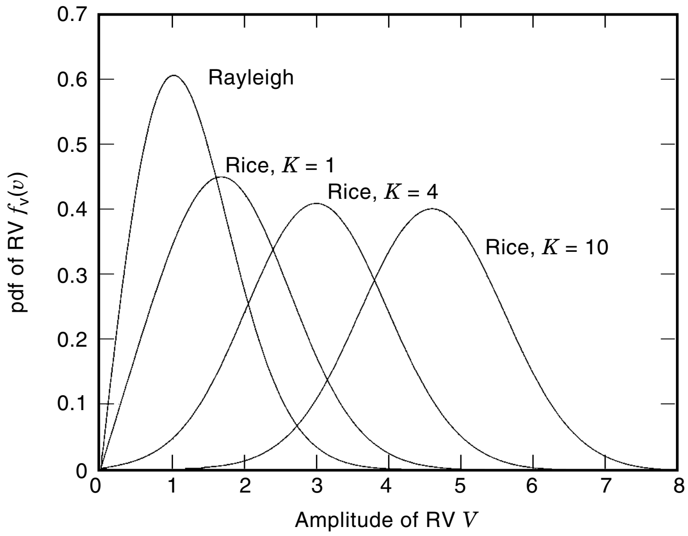


**Figure 6.** Plot of the Rayleigh pdf and the Ricean pdf for different values of the Rice factor $K = 1$, 4, and 10.

A plot of the Ricean pdf for different values of the Ricean factor $K$ is given in Fig. 6. As the value of $K$ increases, the mean (and also the variance) of $V$ increases. In practice, this implies that the LOS signal component is stronger relative to the scattered signal components, and as a result the magnitude of signal fades is reduced. Figure 7 shows segments of Rayleigh and Ricean fading for different values of $K$. For $K$ = 10, in Fig. 7 the fade depth is typically $\leq$ 10 dB, whereas for $K = 1$, signal fades of up to 30 dB are observed.

## Rayleigh Distribution

As shown in the preceding section, the Rayleigh distribution is a special case of the Rice distribution ($K \to 0$ dB). The Rayleigh distribution can also be derived independently from the central chi-square distribution, as shown herein. Let $X$ and $Y$ be two independent identically distributed (iid) zero-mean Gaussian RVs with variance $\sigma^2$. Then the RV $V$ defined as $V \triangleq \sqrt{X^2 + Y^2}$, is distributed according to the *Rayleigh distribution,* whose pdf is given by

$$f_V(v) = \begin{cases} \dfrac{v}{\sigma^2} e^{-\frac{v^2}{2\sigma^2}} & v \geq 0 \\ 0 & v < 0 \end{cases} \tag{11}$$

A brief derivation of the pdf $f_V(v)$ is given in Appendix 1. Equation (11) can be obtained from Eq. (8) by setting $s^2 = 0$. It can also be shown that the RV $\hat{V} = V^2$ has a central chi-square distribution. The cdf of $V$ is given by

$$F_V(v) = Pr(v \leq V) = \int_0^V f_V(v)\, dv = 1 - e^{-\frac{v^2}{2\sigma^2}}, v \geq 0 \tag{12}$$

The mean and variance of $V$ are given by

$$E[V] = \sqrt{\frac{\pi}{2}}\sigma$$

and

$$E[V^2] = 2\sigma^2$$

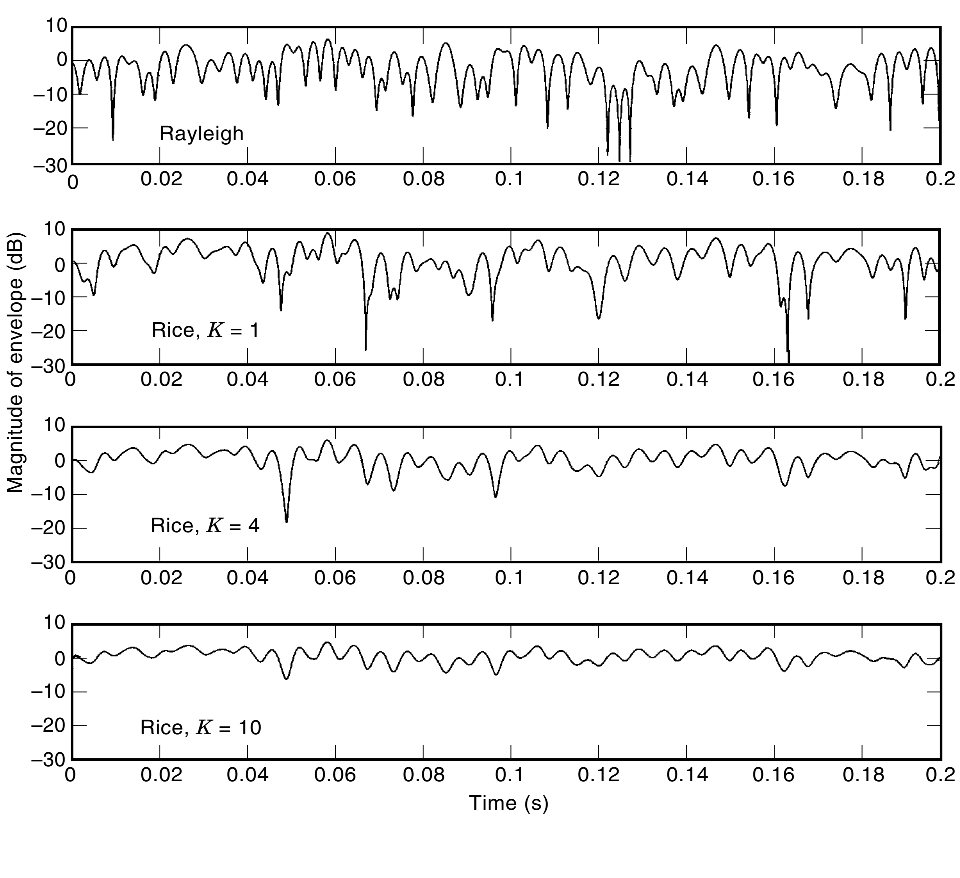


**Figure 7.** Plot of a typical segment of Rayleigh and Ricean fading waveforms.

and the higher order moments of $V$ can be obtained from the expression (4)

$$E[V^k] = (2\sigma^2)^{k/2}\Gamma\left(1+\frac{k}{2}\right)$$

### Nakagami Distribution

The Nakagami-$m$ distribution (5) was designed to fit empirical data and in some cases provides a better match than Rayleigh or Rice distributions. Hence, it is frequently used to characterize the statistical fluctuations of signals transmitted over multipath fading channels. An RV $V$ with *Nakagami-m distribution* has a pdf given by

$$f_V(v) = \frac{2}{\Gamma(m)}\left(\frac{m}{\Omega}\right)^m v^{2m-1}e^{-\frac{mv^2}{\Omega}}, m \geq 1/2 \qquad (13)$$

where $\Omega = E[V^2]$, $\Gamma(m)$ is the gamma function, and the parameter $m$ is called the fading figure, defined as

$$m \triangleq \frac{\Omega^2}{E[(V^2-\Omega)^2]}, \quad m \geq 1/2$$

The following are special cases of the Nakagami-$m$ distribution:

- $m = 1$; the Nakagami-$m$ distribution reduces to the Rayleigh pdf.
- $m = 1/2$; $f_V(v)$ is the one-sided Gaussian pdf (more severe than Rayleigh fading).
- $m \to \infty$; it is a static channel (no fading).
- The Nakagami-$m$ distribution also provides a close approximation of the Rice distribution with the following relationship between the Rice factor $K$ and the Nakagami parameter $m$:

$$m = \frac{(K+1)^2}{(2K+1)}$$

Because of its versatility in modeling a wide range of fading conditions and its analytical tractability, the Nakagami-$m$ distribution is widely used.

### Log-Normal Distribution

The variations in the local mean of the signal power received in a fading environment is referred to as shadowing. These variations are caused by terrain and other environmental factors. Shadowing is characterized via the log-normal distribution, as defined herein. An RV $\Omega'$ is said to have a log-normal distribution if its pdf is given by

$$f(\Omega) = \frac{1}{2\pi\sigma_\Omega}e^{\frac{-(\Omega-\mu)^2}{2\sigma_\Omega^2}} \qquad (14)$$

where

$$\Omega = 20\log_{10}\Omega'$$
$$\mu = E[\Omega]$$

and

$$\sigma_\Omega^2 = E[\Omega^2] - \mu^2$$

## CHARACTERIZATION OF RAYLEIGH FADING

Extensive measurements of the envelope variations of signals have been carried out in the 100 MHz to 2000 MHz frequency band, which covers commercial cellular, public safety, and special mobile radio applications. The measured data confirm that the envelope of the received signal is Rayleigh distributed when measured over short distances ($\sim 10\lambda$–$20\lambda$) over which the mean signal level is constant. In this section, the key results of the mathematical model of Rayleigh fading channels and their characterization are presented. For a complete derivation of the results, the reader is referred to Refs. 1–3. Herein, the model proposed in Ref. 1 is considered.

### Mathematical Model for Rayleigh Fading

In Fig. 8, the $X$–$Y$ plane is assumed to be the horizontal ground plane. Consider a mobile receiver moving with velocity $v$ along the $X$-axis. The model (1) is that the signal received consists of a number of horizontally traveling plane waves each with random amplitude (but equal on average) and random angle of arrival. The phases of the waves are uniformly distributed in $[0, 2\pi]$ and are assumed to be statistically independent of the amplitudes.

Let the angle of the $n$th incoming wave be $\alpha_n$ w.r.t. the $X$-axis. We assume a fixed transmitter with a vertically polarized antenna and a mobile receiver with a whip/monopole antenna. The vehicular motion introduces a Doppler shift given by

$$f_{\mathrm{n}} = \frac{v}{\lambda}\cos\alpha_{\mathrm{n}}\ (\mathrm{Hz}) \qquad (15)$$

where $v$ is the velocity in m/s and $\lambda$ is the wavelength (in meters) of the transmitted carrier signal. From Eq. (15), the maximum Doppler shift is given by $f_{n,\max} = v/\lambda$ Hz.

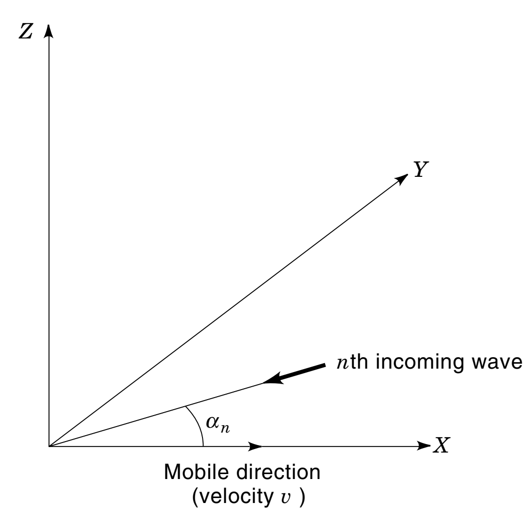


**Figure 8.** Reference figure for deriving the mathematical model for Rayleigh fading.

The electric and magnetic field components received at the mobile receiver are $E_z$, $H_x$, and $H_y$ respectively. Next, the expressions for $E_z$ are derived. The superposition of the different waves is expressed as

$$E_z = E_0 \sum_{n=1}^{N} C_n \cos(2\pi f_c t + \theta_n) \tag{16}$$

where $\theta_n = 2\pi f_n t + \phi_n$, where $f_c$ is the carrier frequency, $f_n$ is the Doppler shift, $E_0C_n$ is the amplitude of the $n$th wave, and $\phi_n$ are the random phase angles uniformly distributed in [0, $2\pi$]. The $C_n$ are normalized such that $\langle \sum_{n=1}^{N} C_n^2 \rangle = 1$, where $\langle\ \rangle$ indicates the ensemble average. For large $N$, using the central limit theorem, the field components $E_z$, $H_x$, and $H_y$ can be approximated by Gaussian random processes. The following derivation assumes that the mean power of the signal is constant with time, which is typically the case as the mobile receiver traverses short distances (i.e., the shadowing is a constant). Equation (16) can be expressed as

$$E_z = T_c(t)\cos 2\pi f_c t - T_s(t)\sin 2\pi f_c t \tag{17}$$

where

$$T_c(t) = E_0 \sum_{n=1}^{N} C_n \cos(2\pi f_n t + \phi_n)$$
$$T_s(t) = E_0 \sum_{n=1}^{N} C_n \sin(2\pi f_n t + \phi_n) \tag{18}$$

Both $T_c(t)$ and $T_s(t)$ are Gaussian random processes. The corresponding RVs $T_c$ and $T_s$ have zero mean and equal variance given by

$$\langle T_c^2 \rangle = \langle T_s^2 \rangle = E_0^2/2$$

and the ensemble average is evaluated over $\alpha_n$, $\phi_n$, and $C_n$. The Gaussian RVs $T_c$ and $T_s$ are uncorrelated and hence independent. Their common variance is $E_0^2/2$. The envelope of $E_z$ is given by

$$|E_z| = V \triangleq \sqrt{T_c^2 + T_s^2} \tag{19}$$

Using the results from the section on Raleigh distribution, $V$ is a Rayleigh distributed random variable, whose pdf is given by Eq. (11).

### Power Spectrum of Rayleigh Fading

If the transmitted signal is a sinusoid of frequency $f_c$, the instantaneous frequency of the received signal arriving at angle $\alpha$ is given by [using Eq. (15)]

$$f(\alpha) = f_c + f_m \cos\alpha \tag{20}$$

where $f_m$ is the maximum Doppler frequency. Hence

$$\cos\alpha = \left(\frac{f - f_c}{f_m}\right)$$

and

$$\sin\alpha = \sqrt{1 - \left(\frac{f - f_c}{f_m}\right)^2} \tag{21}$$

Assuming a large number of scatterers and that the mobile receiver has a vertical whip antenna, then the total incoming power is uniform as a function of the incident angle $\alpha$. Using the derivation in Refs. 1 and 3, the power spectrum of the electric field is given by

$$S_{E_z}(f) = \begin{cases} \dfrac{3b}{2\pi f_m} \dfrac{1}{\sqrt{1 - \left(\dfrac{f - f_c}{f_m}\right)^2}}, & |f - f_c| \le f_m \\ 0 & |f - f_c| > f_m \end{cases} \tag{22}$$

where $b$ is a scale factor denoting the mean power received by an isotropic antenna. A normalized plot of the power spectrum is shown in Fig. 9. The peak of the power spectrum occurs at $\pm f_m$. The power spectra for the magnetic field components are given in Ref. 1.

### Envelope Correlation for Rayleigh Fading

An important result obtained by using the power spectrum $S_{E_z}(f)$ is the envelope correlation $R_{TT}(\tau) = \langle T(t)T^*(t + \tau)\rangle$ where $T(t) = T_c(t) + jT_s(t)$ is the baseband representation of the $E$-field components given by Eq. (18) and the envelope correlation is expressed as a function of the time separation $\tau$. Using the Fourier relationship,

$$\begin{aligned} R_{TT}(\tau) &= \int_{f_c - f_m}^{f_c + f_m} S_{E_z}(f) e^{-j2\pi(f - f_c)\tau}\, df \\ &= \int_{f_c - f_m}^{f_c + f_m} \frac{3b}{2\pi f_m} \frac{e^{j2\pi(f - f_c)t}}{\sqrt{1 - \left(\dfrac{f - f_c}{f_m}\right)^2}}\, df \end{aligned} \tag{23}$$

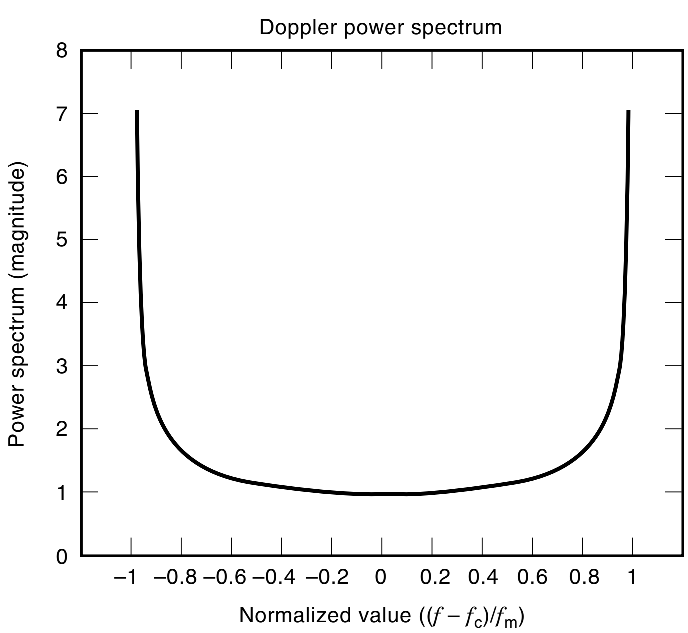


**Figure 9.** Power spectrum of the received $E$-field in a Rayleigh fading environment.

It can be shown that

$$\begin{aligned} R_{\mathrm{TT}}(\tau) &= \langle T_{\mathrm{c}}(t)T_{\mathrm{c}}(t+\tau)\rangle + \langle T_{\mathrm{s}}(t)T_{\mathrm{s}}(t+\tau)\rangle \\ &= \int_{f_{\mathrm{c}}-f_{\mathrm{m}}}^{f_{\mathrm{c}}+f_{\mathrm{m}}} \frac{3b}{2\pi f_{\mathrm{m}}} \frac{1}{\sqrt{1-\left(\dfrac{f-f_{\mathrm{c}}}{f_{\mathrm{m}}}\right)^2}} \cos(2\pi(f-f_{\mathrm{c}})t)\,df \end{aligned} \tag{24}$$

From Ref. 20, we have the result

$$\int_0^1 \frac{1}{\sqrt{1-x^2}} \cos(ax)\,dx = \pi/2J_0(a)$$

where $J_0$ is the zeroth order Bessel function of the first kind. Using this result,

$$R_{\mathrm{TT}}(\tau) = 1.5bJ_0(2\pi f_{\mathrm{m}}\tau) \tag{25}$$

This shows that the envelope of a Rayleigh faded signal has a Bessel autocorrelation function, which plays an important part in designing effective error-correcting coding and interleaving techniques for Rayleigh fading channels.

### Rayleigh Fading Statistics

Two statistical properties that help characterize Rayleigh fading are

1. the level crossing rate (LCR)
2. the duration of fades

The derivation of these two parameters is based on the work of Rice (1,7,8).

**Level Crossing Rate.** The level crossing rate (LCR) is defined as the expected rate at which the Rayleigh fading envelope $V(t)$, normalized to the local rms signal level, crosses a specified level ($V_{\mathrm{ref}}$ in a positive direction. Figure 10 depicts a typical envelope variation which has three crossings of the level $V_{\mathrm{ref}}$ in the duration of $T$ seconds. The LCR $N_V$, the number of level crossings per second is given by (1)

$$N_V = \int_0^\infty \dot{v}p(V,\dot{v})\,d\dot{v} = \sqrt{2\pi} f_{\mathrm{m}}\rho e^{-\rho^2} \tag{26}$$

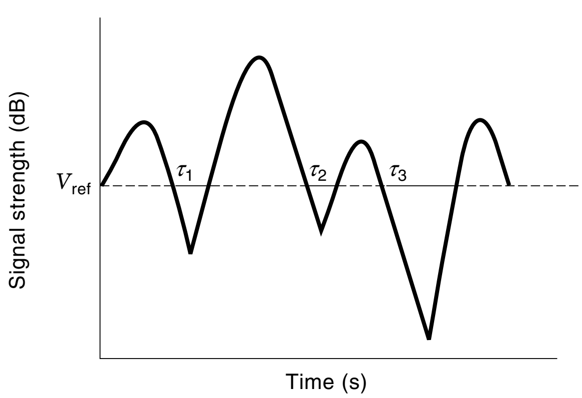


**Figure 10.** A method to compute the level crossing rate and fade duration for Rayleigh fading.

where $\dot{v}$ is the rate of change (the time derivative) of the envelope $V(t)$, $p(V, \dot{v})$ is the joint pdf of $v$ and $\dot{v}$ at a specified value of $V$, and $\rho = V/V_{\mathrm{rms}}$ is the normalized value of the envelope. It can be verified that the peak value of $N_V$ occurs at $\rho = -3$ dB.

***Example 2:*** Consider a signal with carrier frequency of 1.9 GHz and a receiver moving at a velocity of 100 km/ph. The corresponding value of the Doppler frequency $f_{\mathrm{m}} = 176$ Hz. At a normalized value of $\rho = 0$ dB, using Eq. (26), we obtain the value $N_V = 162$ crossings/s. Hence the LCR gives a characterization of the fluctuation rate of the signal envelope.

**Duration of Fades.** The duration of fades is the expected value of the time at which the signal level is below a specified value $V_{\mathrm{ref}}$. In Fig. 10, consider a time interval $T$ (seconds), and let $\tau_i$ be the duration of the $i$th fade below the level $V_{\mathrm{ref}}$. Then

$$P[v \le V] = \frac{1}{T}\sum_i \tau_i \tag{27}$$

Using the expression for the pdf of $V$,

$$P[v \le V] = \int_0^V p(v)\,dv = 1 - e^{-\rho^2} \tag{28}$$

where $\rho = V/V_{\mathrm{rms}}$. Using Eqs. (27) and (28), we obtain the expression for $\overline{T}_{\mathrm{fade}}$, the average duration of a fade below $v = V$ (as given in (1)),

$$\overline{T}_{\mathrm{fade}} = \frac{1}{TN_{\mathrm{V}}}\sum_i \tau_i = \frac{1}{\sqrt{2\pi}} \frac{[e^{\rho^2}-1]}{\rho f_{\mathrm{m}}} \tag{29}$$

***Example 2 (cont'd.):*** Consider the same example as in the preceding section. For the same parameters, using Eq. (29), the average duration of a fade 20 dB below the rms value of the envelope $\rho = 1.43$ ms.

**Observations Based on Fading Statistics.**

- $N_V \propto f_{\mathrm{m}}$ and $\overline{T}_{\mathrm{fade}} \propto 1/f_{\mathrm{m}}$
- At low Doppler frequency, the LCR is low, and hence the duration of fades is long. This observation is helpful in choosing diversity and error-correction schemes over fading channels.
- The value of $\overline{T}_{\mathrm{fade}}$ yields an estimate of the number of symbols that may be lost because of a fade (burstiness of errors caused by fading).

In particular, if a mobile communication system is designed with a specified fade margin, then the performance of the receiver can be estimated by using the parameters $f_{\mathrm{m}}$, $\rho$, and $\overline{T}_{\mathrm{fade}}$ to relate the instantaneous signal to noise ratio (SNR) to the instantaneous bit error rate (BER).

**Random Frequency/Phase Modulation.** The baseband representation of the $E$-field components, as given in Eq. (18), can be expressed as

$$T(t) = T_{\mathrm{c}}(t) + jT_{\mathrm{s}}(t) = A(t)e^{j\phi(t)} \tag{30}$$

where $T_c(t)$ is the in-phase component and $T_s(t)$ is the quadrature component. The effect of the multipath fading channel is represented by $T(t)$, which is a complex-valued, multiplicative scaling of the transmitted signal. The time-varying nature of $T_c(t)$ and $T_s(t)$ manifests itself as a random phase modulation of $\theta(t)$. In FM receivers, the effect of $T(t)$ produces a baseband noise component, which can be evaluated (1). The baseband noise is characterized by the frequency deviation it produces. It is interesting to note that the frequency deviation (and hence, the rms value of the baseband noise) depends on the depth of the fade. As the signal envelope $V$ experiences deep fades, the frequency deviation of the random FM increases proportionally. The effect of $T(t)$ can also be viewed as random phase rotation given by arctan $[T_s(t)/T_c(t)]$. Hence, multipath fading causes impairments of the received signal that have the characteristics of random FM and random phase shifts.

## SIMULATION OF RAYLEIGH FADING

In the preceding sections, the power spectrum and the envelope correlation of a Rayleigh faded signal have been discussed. Using these results, two methods are obtained for generating Rayleigh fading:

1. the stochastic filtered noise approach (9,10)
2. the Jakes method (deterministic) (1)

Both methods are easily modified to generate Ricean fading. Let $T(t) = T_c(t) + jT_s(t)$ be the complex baseband representation of Rayleigh fading. The main requirements on $T_c$ and $T_s$ for generating Rayleigh fading are that

- they have a Gaussian pdf
- they be zero mean and have equal variance (typically normalized to 0.5, such that the variance of $T(t)$ is unity
- $T_c$ and $T_s$ must be uncorrelated
- the autocorrelation of $T(t)$ must satisfy the condition in Eq. (25); This condition also implies that the power spectrum closely approximates Eq. (22).

### Filtered Noise Approach

The method for implementing the stochastic filtered noise approach is shown in Fig. 11. The steps are as follows:

1. Generate two independent Gaussian (white) noise sources.
2. Each of the sequence of random variables (samples of the noise) is filtered by a baseband Doppler filter whose frequency response is given by $\sqrt{S_{E_z}(f)}$.
3. The output of the Doppler filters yields the in-phase and quadrature component of the Rayleigh fading signal.

It can be verified that the output signal $T_c + jT_s$ has a Rayleigh envelope with the time correlation specified by the maximum Doppler frequency $f_m$. The filtering in step 2 can be done in the frequency domain via FFT. The steps for using the FFT for the filtering are outlined in Ref. 9.

### Jakes' Method

In this section, the Jakes approach (deterministic) for generating Rayleigh fading is discussed (Fig. 12). The main advantage of this method over the stochastic method is that segments of time-correlated fading can be generated without having to generate the fading in between the desired segments, as is typically the case when simulating the performance of Time Division multiple access (TDMA) signals.

The details of the model (Fig. 12) are as follows:

- There are $N_0$ oscillators with frequencies given by

$$f_n = f_m \cos\left(\frac{2\pi n}{N}\right), n = 1, 2, \ldots, N_0 \quad (31)$$

  and one oscillator with frequency $f_m$, where $f_m$ is the maximum Doppler frequency. The total number of oscillators is $(N_0 + 1)$, where $N_0 = \frac{1}{2}(N/2 - 1)$. The parameter $N$ is chosen such that $T_c$ and $T_s$ are Gaussian and the power spectrum of $T(t) = T_c(t) + jT_s(t)$ closely approximates the condition in Eq. (22). In Ref. (1), it is shown that a good approximation is obtained for $N > 34$ ($\Rightarrow N_0 \geq 8$).
- In Fig. 12, the phases $\alpha$ and $\beta_n$, $n = 1, 2, \ldots, N_0$ are chosen such that the probability distribution of the resultant phase (arg[$T(t)$]) is close to a uniform distribution in $[0, 2\pi]$. These phases are introduced by the respective multipliers 2 cos $\beta_n$ and 2 sin $\beta_n$. The uniform distribution of arg[$T(t)$] is ensured if

$$\langle T_c^2 \rangle = \langle T_s^2 \rangle$$

  and

$$\langle T_c T_s \rangle = 0 \quad (32)$$

Choices of values that satisfy Eq. (32) are

$$\alpha = 0$$
$$\beta_n = \frac{\pi n}{N_0 + 1}$$
$$Scale1 = \frac{1}{\sqrt{2N_0}}$$
$$Scale2 = \frac{1}{\sqrt{2(N_0 + 1)}}$$

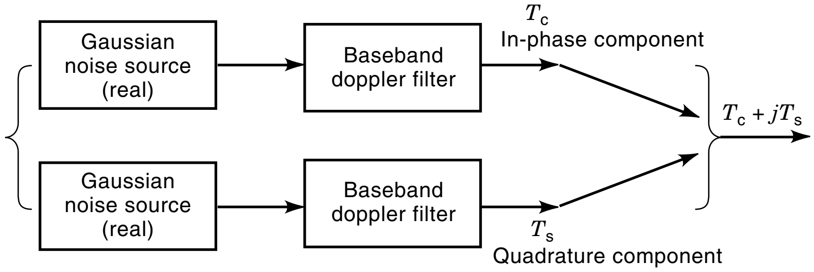


**Figure 11.** Stochastic filtered noise method for generating Rayleigh fading.

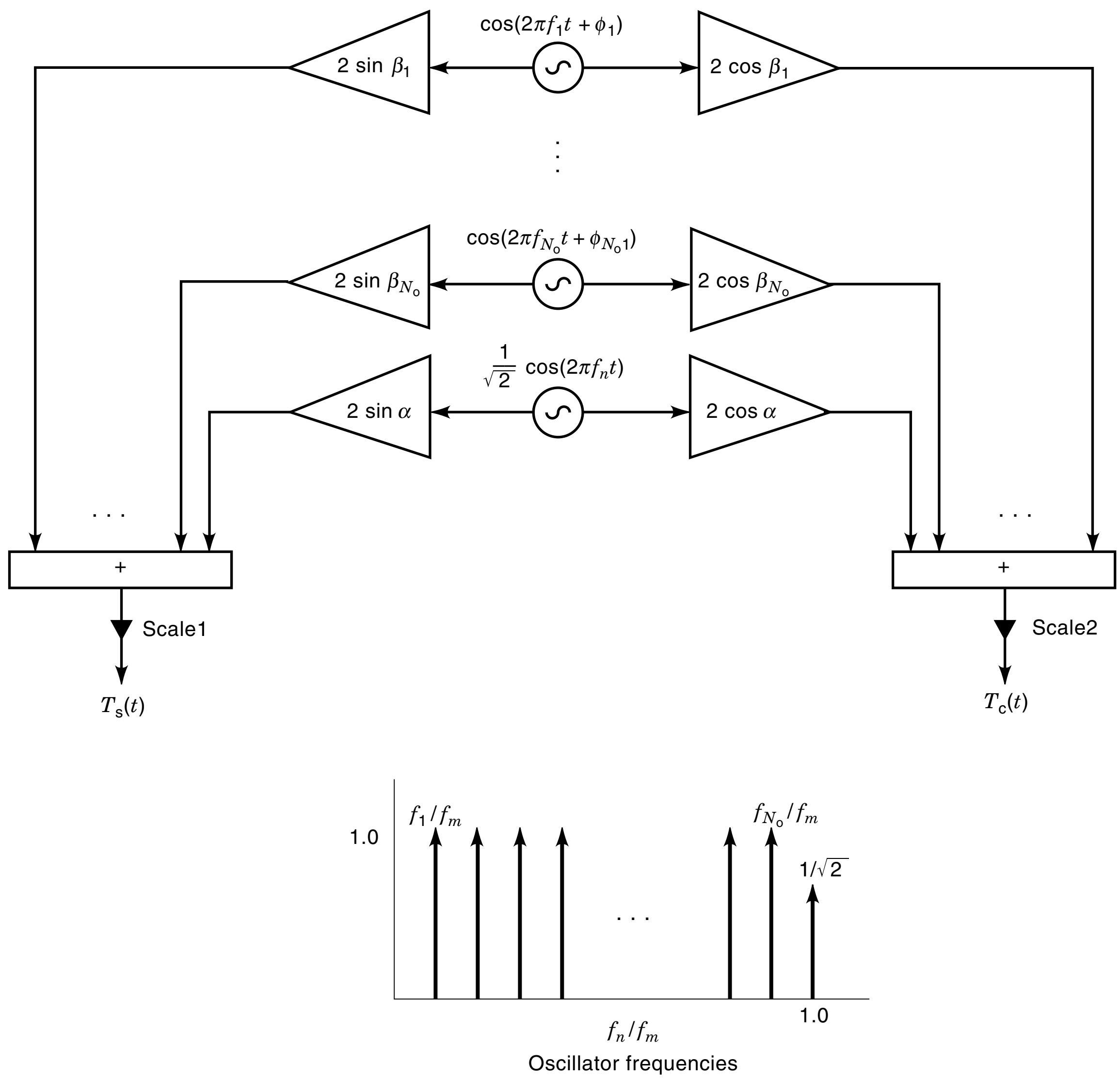


**Figure 12.** Jakes' method for generating Rayleigh fading.

Other choices are also possible.

- The oscillator phases $\phi_n$ in Fig. 12 are randomly chosen in the range [0, $2\pi$]. The purpose of $\phi_n$ is to provide a means of randomly initializing the fading waveform generator. They do not affect the statistical properties of $T_c(t)$ and $T_s(t)$.

### Generating Multiple Uncorrelated Fading Waveforms

In many practical applications, it is necessary to generate multiple uncorrelated Rayleigh fading waveforms. In Ref. 1, a method of modifying Fig. 12 to generate multiple uncorrelated fading is mentioned. However, it has been observed (11) that the method in Ref. 1 produces waveforms with nonzero correlation when more than two waveforms are generated. An attractive and computationally efficient alternative is presented in (11) based on the Walsh–Hadamard transform. Using this method, the multiple fading waveforms are guaranteed to be uncorrelated.

## CHARACTERIZATION OF MULTIPATH CHANNELS

Consider the equivalent, complex-valued, low-pass impulse response of a time-varying multipath channel $c(\tau;t)$ as given by Eq. (5), where $c(\tau;t)$ is a zero-mean, complex-valued Gaussian random process in the variable $t$. Assume that $c(\tau;t)$ is wide sense stationary (WSS). Then the autocorrelation of $c(\tau;t)$ is given by

$$\phi_c(\tau_1, \tau_2; \Delta t) = \frac{1}{2} E[c(\tau_1; t)c^*(\tau_2; t + \Delta t)] \tag{33}$$

Assuming uncorrelated scattering, that is, that the scattering/multipath signal at delay $\tau_1$ given by $c(\tau_1;t)$ is uncorrelated to the signal at delay $\tau_2$ given by $\tau_2$ given by $c(\tau_2;t)$, hence,

$$\phi_c(\tau_1, \tau_2; \Delta t) = \phi_c(\tau_1; \Delta t)\delta(\tau_1 - \tau_2) \tag{34}$$

When $\Delta t = 0$, $\phi_c(\tau, 0) = \phi_c(\tau)$, which is called the *multipath intensity profile,* or the *power-delay profile.* There are different experimental methods for measuring the power-delay profile of a channel such as direct pulse measurement, spread spectrum sliding correlator measurement, and frequency-domain channel sounding (10). A typical power-delay profile is given in Fig. 14. The range of $\tau$ over which $\phi_c(\tau)$ is nonzero is called the *multipath spread* of the channel $\tau_m$.

**Time-Dispersion Parameters.** The mean excess delay, rms delay spread, and the excess delay spread are channel parameters that are obtained from the power-delay profile $\phi_c(\tau)$.

- The *mean excess delay* of the power-delay profile is given by

$$\overline{\tau} = \frac{\sum_k \phi_c(\tau_k)\tau_k}{\sum_k \phi_c(\tau_k)} \tag{35}$$

  where $\phi_c(\tau_k)$ is the strength of the multipath component with delay $\tau_k$ (obtained from the power-delay profile). Typically the $\tau_k$ are measured relative to the first arriving multipath signal.
- The *rms delay spread* is defined as $\sigma_\tau = \sqrt{\overline{\tau^2} - (\overline{\tau})^2}$, where $\overline{\tau^2}$ is given by

$$\overline{\tau^2} = \frac{\sum_k \phi_c(\tau_k)\tau_k^2}{\sum_k \phi_c(\tau_k)} \tag{36}$$

- Suppose that $\tau_0$ is the first arriving multipath and $\tau_K$ is the delay beyond which the power drops below $X$ dB of the maximum strength multipath component, then, $(\tau_K - \tau_0)$ is called the maximum excess delay ($X$ dB).

In practice, the value of $\overline{\tau}$, $\overline{\tau^2}$, and $\sigma_\tau$ depend on the value of the threshold for detecting the presence of a signal component.

**Coherence Bandwidth.** The coherence bandwidth $B_c$ is an important parameter in time-dispersive channels. $B_c$ can be viewed as the range of frequencies over which there is a strong envelope correlation. There is, however, more than one formal definition of $B_c$. In Ref. 4, the coherence bandwidth is defined as the reciprocal of the multipath spread of the channel $\tau_m$,

$$B_c \approx \frac{1}{\tau_m} \tag{37}$$

A more widely used engineering definition of $B_c$ is given in Refs. 1, 7, 10, and 12. Wherein the coherence bandwidth is defined as the bandwidth over which the frequency correlation is $>0.5$. In Ref. 12 it is shown that to satisfy this condition,

$$B_c \approx \frac{1}{2\pi\sigma_\tau} \approx \frac{1}{6\sigma_\tau} \tag{38}$$

where $\sigma_\tau$ is the rms delay spread given by Eq. (36). Another interpretation of $B_c$ is as follows. If two sinusoids with frequency separation $>B_c$ are transmitted through this channel, then they are affected differently. For modulated signals, if $B_c$ is smaller than the BW of the signal($W$), then the channel is said to be *frequency-selective.* If $B_c$ is greater than the BW of the signal, the channel is said to be *frequency-nonselective.*

**Coherence Time.** The rms delay spread ($\sigma_\tau$) and the coherence BW ($B_c$) describe the time-dispersive nature of the channel. Analogously, the Doppler spread ($B_D$) and the coherence time ($T_c$) describe the time-varying nature of the channel in a local area (small-scale region). The Doppler spread $B_D$, is defined as the range of frequencies over which the Doppler spectrum is nonzero. In Ref. 4, the coherence time is defined as

$$T_c \approx \frac{1}{B_D} \tag{39}$$

Coherence time is a measure of the length of time over which the channel impulse response is essentially constant. Alternatively, the coherence time can be viewed as the length of time over which two received signals have a strong potential for envelope correlation. Just as coherence BW has a statistical definition, coherence time $T_c$ can be defined (12) as the time over which the time correlation function is $\geq 0.5$. In Ref. 12 it is shown that

$$T_c \approx \frac{9}{16\pi f_m} \tag{40}$$

where $f_m$ is the maximum Doppler frequency.

### Channel Classification

Multipath fading channels are classified on the basis of the way the channel appears to the transmitted signal. The coherence bandwidth $B_c$ and the coherence time $T_c$, two of the main properties that influence the effect of the channel on the transmitted signal, are classified as follows:

- If the BW of the transmitted signal ($W$) is smaller than the coherence BW ($B_c$), then the fading channel appears as *frequency-nonselective* or *frequency flat.* This implies that all the frequencies of the transmitted signal experience the same channel effects. If $W = B_c$, then it is classified as frequency selective fading channel.
- If the duration of the received waveform [a symbol duration ($T_s$) for digital transmission) is less than the coherence time, then the channel is said to be *time flat*. Otherwise, it is classified as time-selective.

Based on these definitions, we have the classification depicted in Fig. 13.

### A Tapped-Delay Line Channel Model

In addition to providing channel information such as the rms delay spread, the power-delay profile $\phi_c(\tau)$, also provides a means for modeling the channel using a tapped-delay line (FIR) model. From Eq. (5), $\alpha_n(t)$ is the amplitude/gain coefficient for a path arriving with delay $\tau_n(t)$. A typical power-delay profile is shown in Fig. 14, which in the second figure, is uniformly sampled into equal delay bins. In general, the different bins contain a number of received signals (corresponding to different paths) whose times of arrival lie within the particular delay bin. These signals are represented by an impulse at the center of each delay bin that has an amplitude with the appropriate statistical distribution (Rayleigh, Ricean, etc.). In deriving this model, two assumptions are made:

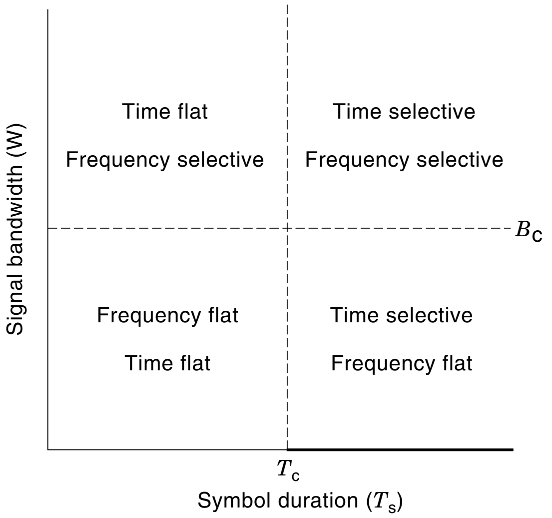


**Figure 13.** A typical power delay profile and the method of sampling the power delay profile to generate a tapped-delay line model.

- there are sufficient number of rays clustered together in each delay bin;
- the statistical distribution of the envelope is known.

The rate of sampling the power-delay profile is affected by the time resolution desired and also the bandwidth of the transmitted signal. The next step after sampling the power-delay profile is to use a threshold (say $X$ dB below the peak of the power-delay profile), and using the threshold to truncate those samples below the threshold. This model can be implemented by using a tapped-delay line or FIR model, thereby allowing us to model any arbitrary channel.

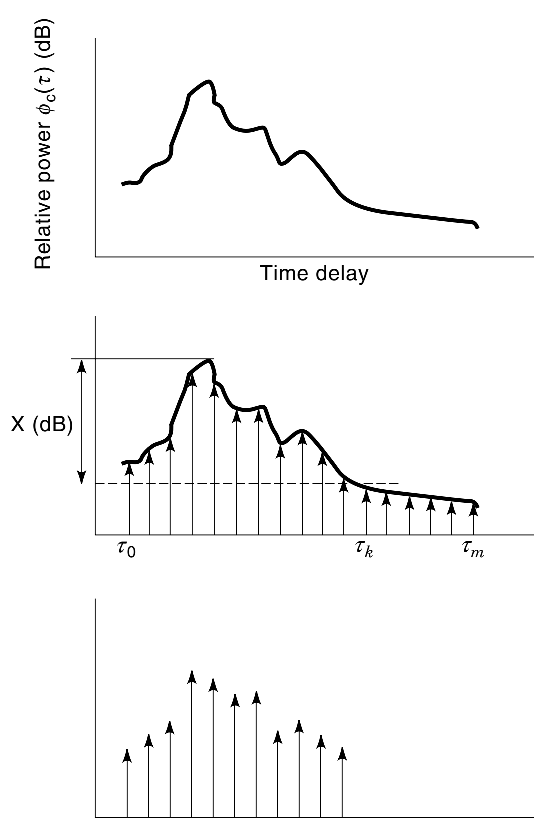


**Figure 14.** Classification of multipath fading channels.

## LARGE-SCALE EFFECTS

Understanding and characterizing the effects of the RF propagative channel are essential to designing RF communication systems. A wide range of channel conditions are encountered in RF communications, all the way from LOS channels to severely obstructed channels. Further, the channel may also be time-varying. Hence modeling is based on statistical and experimental information. This is an area of extensive research and measurements, over the past two decades, and even until the present time (1,7,10,16–20). In this section, the two main components of signal variability due to the large-scale effects of RF propagation, namely, path loss and shadowing, are discussed.

### Radio Signal Propagation

The salient features of RF propagation are briefly described in this section. For a detailed treatment of this subject, the reader is referred to Refs. 7 and 10. The three basic propagative mechanisms, illustrated in Fig. 15, are reflection, diffraction, and scattering. Together, these three modes enable us to estimate the signal level received by a transmitter for a given RF propagative channel.

- *Reflection:* occurs when a radio wave propagating in one medium is incident upon another medium that has different electrical properties and a part of the energy is reflected back into the first medium, depending on the specific electrical properties of the second medium. If the second medium is a perfect conductor, all of the incident energy is reflected. If the second medium is a dielectric, then the energy is only partially reflected. The reflection coefficient is a function of the medium's properties, the signal frequency, and the angle of incidence. Reflections of RF signals typically occur from objects in the propagative path whose size is larger than the wavelength ($\lambda$) of the RF carrier, such as buildings and walls. In the case of cellular/PCS signals at 1.9 GHz, the wavelength $\lambda$ =

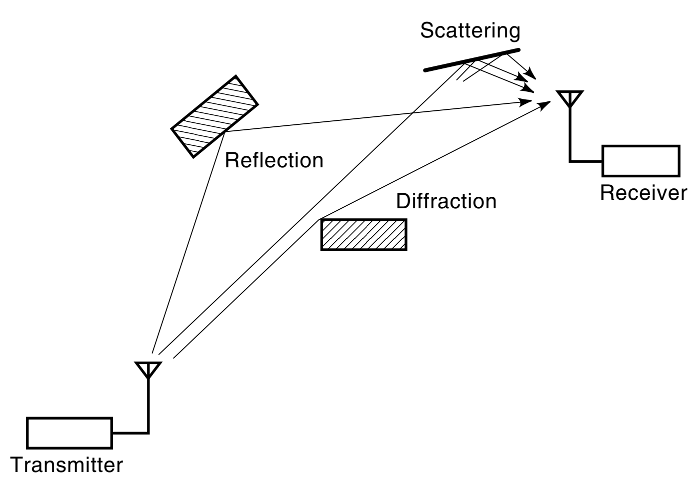


**Figure 15.** The different modes of RF signal propagation, reflection, diffraction, and scattering.

15 cm ≈ 6 in. Hence, a variety of objects act as reflectors. Signals are also reflected from the ground. A model commonly used to characterize RF channels is the two-ray ground reflection model (10).

- *Diffraction:* can be viewed as the "bending" of RF signals around an obstruction, as shown in Fig. 15. Diffraction occurs when the obstruction between the transmitter and receiver has sharp edges. As explained by Huygen's principle, when a wavefront impinges on an obstruction, then secondary wavelets are produced, which give rise to bending of waves around the obstruction. The field strength of the diffracted wave in the shadowed region is the vector sum of the electric field components of the secondary wavelets. The knife-edge diffraction model (10) can be used to characterize the diffraction caused by a single object, such as building in the path of an RF signal.
- *Scattering:* occurs when the RF signal is incident on a surface that has a certain degree of "roughness" (7,10). Scattering in an RF channel is commonly caused by objects, such as buildings. The *critical height* $h_c = \lambda/8 \sin \theta_i$, where $\theta_i$ is the angle of incidence. This implies that the maximum to minimum level of the surface must be greater than $h_c$.

## Propagative Path Loss Models

**Free-Space Propagative Loss.** When there is a LOS path between the transmitter and receiver, the free-space propagation model can be used to predict the signal strength. Such conditions occur in some satellite and terrestrial microwave communication links. Suppose that the distance between the transmitter and receiver is $d$ meters, where $d$ is in the far field. Then the free-space model (based on the Friis formula) gives

$$P_r(d) = \left[\frac{P_t G_t G_r \lambda^2}{(4\pi)^2 L}\right]\frac{1}{d^2} \tag{41}$$

where $P_t$ and $P_r$ are the transmitting and receiving power, respectively, with transmitting antenna gain $G_t$, receiving antenna gain $G_r$, and $\lambda$ is the wavelength of the carrier. The term $L$ represents the losses in the system ($L \geq 1$). The path loss $L_p$ is the difference between the transmitting and receiving power expressed in decibels.

$$L_p(\text{dB}) = 10\log_{10}\frac{P_t}{P_r} = 10\log_{10}\left[\frac{(4\pi)^2 L}{P_t G_t G_r \lambda^2}\right] + 20\log d \tag{42}$$

As the signal propagative distance $d$ increases, the received power decreases at 20 dB/decade, as seen from Eq. (42). Another commonly used method to compute the signal power received $P_r(d)$ is by measuring it relative to the received power $P_r(d_0)$ at a reference point (distance $d_0$ from the transmitter) as given by

$$P_r(d) = P_r(d_0)\left(\frac{d_0}{d}\right)^2,\ d \geq d_0 \tag{43}$$

**Outdoor Propagative Loss.** In dealing with non-LOS environments, which is typical of most RF communication links, such as cellular/PCS, we need appropriate models for computing the propagative path loss (because the criteria for free-space propagation are not met). This topic has been very extensively studied. Detailed information can be found in Refs. 7, 10, 12, and 16. Computation of path loss is of particular interest to communication systems designers. Because the actual RF communication environments encountered in practice are so numerous, a unified theoretical/analytical framework for estimating path loss is not feasible. Most system designers resort to empirical approaches and semianalytical methods, which have been validated by experimental/measured data, to estimate the path loss. The work of Okamura and Hata (13) is very widely used for path loss estimation. Okamura's work is based purely on measured data, and Hata provided the empirical model to fit that data. The advantage of using empirical models and curve fitting to measured data is that it accounts for both known and unknown sources of path loss. On the other hand, the disadvantage is that the validity of the empirical model, derived from a set of data, is not guaranteed for a different environment.

Let $d$ be the distance between the transmitter and receiver. Both theoretical and measurement-based models show that the average path loss $[L_p(d)]$ increases directly proportional to $d^n$, where $n$ is called the path loss exponent. Typically $n \geq 2$, as summarized in the Table 1. By contrast, in free space, $N = 2$. The path loss $L_p(d)$ is given by

$$L_p(d) \propto d^n \tag{44}$$

$$L_p(d) = L_p(d_0) + 10n\log_{10}\left(\frac{d}{d_0}\right) \tag{45}$$

The reference point $d_0$ is chosen such that $L_p(d_0)$ can be computed using the free-space path loss model.

**Hata and COST-231 Models.** This is one of the most widely used models for estimating path loss in RF communication channels. Based on extensive measured data, Okamura generated sets of curves that characterize the median attenuation (50th percentile) $L_{p,50}$, for a wide range of environments (range of carrier frequency ($f_c$), effective height of transmitting antenna ($h_{t,\text{eff}}$), and distance $d$ from transmitter. Hata (12) provided an empirical formulation from Okamura's data, which shows good agreement (between the model and the measured data) for $f_c \leq 1.5$ GHz. An extension of Hata's model for frequencies up to 2 GHz is provided in Ref. 14. The Hata model and COST-231 models are given below: Hata Model

$$L_{p,50} = 69.55 + 26.16\log_{10} f_c - 13.82\log_{10} h_{t,\text{eff}} - a(h_{r,\text{eff}}) + (44.9 - 6.55\log_{10} h_{t,\text{eff}})\log_{10} d \tag{46}$$

**Table 1. Path Loss Exponents for Different Environments**

| Environment | Path Loss Exponent $n$ |
|---|---|
| Free space | 2 |
| Urban cellular | 2.7-4.0 |
| In-building (non-LOS) | 3.0-6.0 |
| Shadowed urban cellular | 4.0-6.0 |

COST-231 Model

$$L_{p,50} = 46.3 + 33.9\log_{10} f_c - 13.82\log_{10} h_{t,\mathrm{eff}} - a(h_{r,\mathrm{eff}}) + (44.9 - 6.55\log_{10} h_{t,\mathrm{eff}})\log_{10} d + C_M \quad (47)$$

where $h_{r,\mathrm{eff}}$ is the effective height of the receiving antenna, $a(h_{r,\mathrm{eff}})$, is a correction factor based on $h_{r,\mathrm{eff}}$ and $C_M$ is a correction factor based on the propagative environment. The details regarding $a(h_{r,\mathrm{eff}})$, and $C_M$ are provided in Ref. 10. The range of values for which the Hata and COST-231 models are valid are summarized in Table 2.

The Hata model has a correction factor for rural environments. In general, the Hata model and the COST-231 model provide an example of the path loss computation in a outdoor, non-LOS environment. A variation, called the COST231-Walfish–Ikegami model can be used for transmitting antennas above or below rooftops and is accurate for $d > 20$ m. A number of models similar to these discussed in this section are also used in practice. So, the choice of path loss models must take into account all aspects of the propagative environment, including transmission frequency, distance of transmission, polarization, antenna heights, surface refractivity, terrain irregularity, foliage, climate, ground conductivity, and ground dielectric constant (10).

**Indoor Propagative Loss.** An increasing number of wireless communications applications are designed for indoor environments. Hence, there is considerable interest in indoor propagation and in models for it. Although the characteristics of indoor propagation vary slowly [quasi-static behavior (15)] as compared with outdoor propagation, a key difference is that propagation within a building is strongly influenced by a number of factors, such as building type, layout, construction material (amount of metal used), types of partitions, and height and placement of antennas. As a result, the variability in signal propagation and hence the path loss is quite significant. The model best suited for characterizing path loss in indoor propagation is similar to that for log-normal shadowing. The path loss at a distance $d$ from the transmitter is given by

$$L_p(d) = \left[L_p(d_0) + 10n\log_{10}\left(\frac{d}{d_0}\right) + \Omega\right](dB) \quad (48)$$

where $\Omega$ is a normal RV with standard deviation $\sigma$ and $n$ is the path loss exponent. It was reported in Ref. 15 that the typical range of $n$ is 3 to 4. A comprehensive list of the typical values of $n$ and $\sigma$ for a variety of indoor environments is provided in Ref. 10.

**Table 2. Range of Validity of Hata and COST-231 Models**

| Parameter | Range of Validity: Hata | COST-231 |
|---|---|---|
| Carrier frequency $f_c$ | 150-1500 MHz | 1500-2000 MHz |
| Effective transmit height $h_{t,\mathrm{eff}}$ | 30-200 m | 30-200 m |
| Effective receive height $h_{r,\mathrm{eff}}$ | 1-10 m | 1-10 m |
| Distance $d$ from transmitter | ≥1 km | 1-20 km |
| Correction factors | $a(h_{r,\mathrm{eff}})$ | $a(h_{r,\mathrm{eff}})$, $C_M$ |

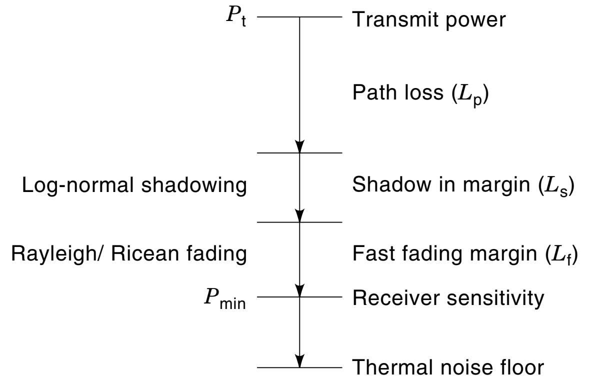


**Figure 16.** Different components of link budget:—propagative loss, shadowing margin, and fading margin.

### Shadowing

As discussed earlier, shadowing is caused by terrain and other environmental factors, such as foliage. The effect of shadowing causes the variations in the mean of the received signal. Let $\hat{L}_p(d)$ denote the path loss (including the effect of shadowing) at a specified distance from the transmitter. Based on extensive measurements, it has been verified that $\hat{L}_p(d)$ can be characterized as a random variable with a log-normal distribution about the mean value. When expressed in dB, the RV perturbing the local mean value of the path loss is a normal RV, as given by

$$\hat{L}_p(d) = [L_p(d) + \Omega](dB) \quad (49)$$

where $L_p(d)$ is given by one of the path loss models in the preceding section and $\Omega$ is a normal RV with standard deviation $\sigma$. The RV $\Omega$ is obtained from the log-normal RV $\Omega'$, whose pdf is given earlier. Equation (49) describes the path loss for a specified value of $d$ but with different values of shadowing/obstructions between the transmitter and receiver. In practice, the path loss exponent $n$ and the standard deviation $\sigma$, are used to characterize any environment. In most cases, $n$ and $\sigma$ can be calculated from measurements.

### A Practical Design Model

The goal of this section is to provide a framework for combining the various results in this article relating to small-scale signal variations and large-scale signal variations into a set of relevant parameters that may be used by communication systems designers for link budget calculations. The components of the different effects and their impact on the link budget are shown pictorially in Fig. 16.

Predicting the expected mean received signal power is an important step in designing a communication link and in estimating the coverage area for a specific transmitter. In Fig. 16, $P_t$ is the transmitted signal power and $P_{min}$ is the minimum signal strength that must be received for the receiver to operate satisfactorily, that is, the signal strength to produce the minimum carrier-to-noise ratio ($C/N$) needed for acceptable communications. This is called *receiver sensitivity* and is expressed in dBm. There are three margins, one for each of the following practical effects:

- propagative path loss
- small-scale effects—fading margin
- large-scale effects—shadowing margin

In the previous section, the methods of determining the path loss $L_p$ for different environments were presented. The large-scale effect due to shadowing is modeled as a log-normal random variable. Hence, a shadowing margin $L_s$ must be included in the link budget (Fig. 16). The small-scale effects, characterized by Rayleigh/Ricean fading cause significant amplitude variations. Hence a fading margin $L_f$ is also included in the link budget. From Fig. 16, the total transmitted power is given by

$$P_t = P_{min} + L_f + L_s + L_p \tag{50}$$

The path loss $L_p$ is deterministic (based on the distance between the transmitter and receiver), whereas the fading and shadowing are probabilistic. The amount of margin must be judiciously chosen so that the net margin is minimized but still meets the minimum signal strength requirements. If the amount of losses exceeds the margin of a communication system, then an *outage* occurs, which implies that the communication link cannot be used until the channel conditions improve. This summarizes the tradeoffs that must be handled by the designers of communication systems.

## CONCLUSION

A comprehensive overview of the RF signal variations related to propagation in multipath fading channels has been presented. The diverse phenomena that cause signal variations are described via mathematical models. The different types of fading and their salient features are discussed in detail. This article provides a mathematical and an engineering-oriented treatment of multipath fading, thereby providing the reader with the necessary tools and the information to understand the different RF propagative issues and the way they affect wireless communication.

## APPENDIX

### Derivation of Rayleigh pdf

Let $X$ and $Y$ be two independent identically distributed (iid) zero-mean Gaussian RVs with variance $\sigma^2$. Because $X$ and $Y$ are independent, their joint pdf is the product of their marginal pdf's:

$$F_{X,Y}(x,y) = \frac{1}{2\pi\sigma^2} e^{-\frac{x^2+y^2}{2\sigma^2}} \tag{51}$$

Using a change of variables, $V \triangleq \sqrt{X^2+Y^2}$ and $\phi \triangleq \tan^{-1}(Y/X)$, the joint pdf $f_{V,\Theta}(v, \theta)$ is given by

$$f_{V,\Theta}(v,\theta) = \frac{f_{X,Y}(x,y)}{|\det \boldsymbol{J}(x,y)|} = \frac{v}{2\pi\sigma^2} e^{-\frac{v^2}{2\sigma^2}} \tag{52}$$

where $\boldsymbol{J}(\boldsymbol{x},\boldsymbol{y})$ is the Jacobian matrix for the transformation of variables. From Eq. (52), we obtain the marginal pdf of $V$ and $\Theta$ as

$$f_\Theta(\theta) = \int_0^\infty f_{V,\Theta}(v,\theta)\,dv = \frac{1}{2\pi} \tag{53}$$

$$f_V(v) = \begin{cases} \dfrac{v}{\sigma^2} e^{-\frac{v^2}{2\sigma^2}} & v \geq 0 \\ 0 & v < 0 \end{cases} \tag{54}$$

Hence, $\Theta$ is uniformly distributed, and $V$ is Rayleigh distributed.

## BIBLIOGRAPHY


1. W. C. Jakes, *Microwave Mobile Communications,* New York: Wiley, 1974.
2. R. H. Clarke, A statistical theory of mobile-radio reception, *The Bell Syst. Tech. J.,* **47**: 957–1000, 1968.
3. M. J. Gans, A power-spectral theory of propagation in the mobile-radio environment, *IEEE Trans. Veh. Technol.,* **VT-21**: 27–38, 1972.
4. J. G. Proakis, *Digital Communication,* 3rd ed., New York: McGraw-Hill, 1995.
5. M. Nakagami, The *m* distribution: A general formula of intensity distribution of rapid fading, in W. G. Hoffman (ed.), *Statistical Methods in Radio Wave Propagation,* New York: Pergamon, 1960, pp. 3–36.
6. I. S. Gradshteyn and I. M. Ryzhik, *Table of Integrals, Series, and Products,* Orlando, FL: Academic Press, 1980.
7. W. C. Y. Lee, *Mobile Communications Engineering,* New York: McGraw-Hill, 1982.
8. S. O. Rice, Statistical properties of a sine wave plus random noise, *The Bell Syst. Tech. J.,* **27**: 109–157, 1948.
9. J. I. Smith, A computer generated multipath fading simulation for mobile radio, *IEEE Trans. Veh. Technol.,* **VT-24**: 39–40, 1975.
10. T. S. Rappaport, *Wireless Communications: Principles and Practice,* New York: IEEE Press, 1996.
11. P. Dent, G. E. Bottomley, and T. Croft, Jakes' fading model revisited, *Electron. Lett.,* **29**: 1162–1163, 1993.
12. R. Steele, *Mobile Radio Communications,* New York: IEEE Press, 1995.
13. M. Hata, Empirical formula for propagation loss in land mobile radio services, *IEEE Trans. Veh. Technol.,* **VT-29**: 317–325, 1980.
14. COST 231, *Urban Transmission Loss Models for Mobile Radio in the 900- and 1800-MHz Bands,* COST 231 TD(90) 119, Revision 2, The Hague, September 1991.
15. A. Saleh and R. A. Valenzuela, A statistical model for indoor multipath propagation, *IEEE J. Selected Areas Commun.,* **SAC-5**: 128–137, 1987.
16. G. L. Stüber, *Principles of Mobile Communications,* Boston: Kluwer, 1996.
17. G. A. Arredondo and J. I. Smith, Voice and data transmission in a mobile radio channel at 850 MHz, *IEEE Trans. Veh. Technol.,* **VT-26**: 88–93, 1977.
18. C. Loo and N. Secord, Computer models for fading channels with applications to digital transmission, *IEEE Trans. Veh. Technol.,* **VT-40**: 700–707, 1991.
19. G. A. Arredondo, W. H. Chriss, and E. H. Walker, A multipath fading simulator for mobile radio, *IEEE Trans. Veh. Technol.,* **VT-22**: 241–244, 1973.
20. GSM Series 03.30.


R. D. KOILPILLAI
Ericsson, Inc.